



Chemical and electrochemical properties of an Oxisol–Ultisol transition in the state of São Paulo, Brazil

Aline R. Coscione^{a,*}, Antonio C. Moniz^{a,1}, Daniel Vidal Pérez^b,
Márcia M.C. Ferreira^c, Otávio A. Camargo^a

^a*Centro de Pesquisa e Desenvolvimento de Solos e Recursos Ambientais, Instituto Agrônomo de Campinas, 13001-970, Campinas-SP, Brazil*

^b*Centro Nacional de Pesquisas de Solos, EMBRAPA, 22460-000, Rio de Janeiro-RJ, Brazil*

^c*Instituto de Química-Universidade Estadual de Campinas, CP 6154, 13084-971, Campinas, Brazil*

Received 18 June 2003; received in revised form 3 September 2004; accepted 22 October 2004

Available online 19 November 2004

Abstract

Soil formation factors such as lateral and base water flows promote the Oxisol–Ultisol transformation on hillslopes in colluvium material with oxic properties. Chemical and electrochemical processes occur simultaneously with the morphological transformation of the soil structure from very fine granular to blocky soil. Statistical analysis techniques, such as principal component analysis (PCA) and hierarchical cluster analysis (HCA), were used to analyze the data collected from two sites in the state of São Paulo, Brazil, allowing a comprehensive description of the processes that entailed the transformation of an oxic horizon to a kandic horizon. The modeling power and the discriminating power from the soft independent modeling of class analogy (SIMCA) method were employed to find which attributes were essential to explain the transformation of an oxic into an argillic horizon. The following attributes were used to describe the processes in the toposequences studied: (a) index of silica reactivity (ISR); (b) index of silica saturation (ISS); (c) ratio of iron extracted with ammonium oxalate, DCB and H₂SO₄; (d) ratio of aluminum extracted with ammonium oxalate, DCB and H₂SO₄; (e) specific surface area (SSA); (f) point of zero salt effect (PZSE); and (g) surface net charge (σ).

© 2004 Elsevier B.V. All rights reserved.

Keywords: Oxic; Kandic; Point of zero salt effect (PZSE); Index of silica reactivity (ISR); Index of silica saturation (ISS); Statistical analysis

1. Introduction

The identification of a particular set of properties that are consistently indicative of soil development is difficult, especially when highly weathered soils, typical in the Brazilian landscape, are involved because of its apparent homogeneity (Moniz and

* Corresponding author. Fax: +55 19 3232 8488.

E-mail address: aline@iac.sp.gov.br (A.R. Coscione).

¹ In memoriam.

Buol, 1982; Curi and Franzmeier, 1984; Cunha et al., 1998). In that case, pedogenesis along a toposequence is most clearly identified by soil morphology and the presence of some features like dense horizons.

Despite this, a few papers have shown that some physico-chemical attributes of soil could be useful for characterization. Hendershot and Lavkulich (1978) and Pérez et al. (1993) succeeded in the use of some electrochemical properties to assess pedogenic development in weathered soils. Gallez et al. (1977) and Herbillon et al. (1977) developed two indexes, based on silica solubility/adsorption, to describe pedogenetic environments resulting from processes of silication/desilication, which have been recognized as important processes for the genesis of soils in the tropics (Curi and Franzmeier, 1984; Anjos et al., 1998; Schaefer et al., 2002).

Thus, the main objective of the present work is to highlight the pattern of some physico-chemical property variations associated with pedons distributed along two well-studied Oxisol–Ultisol toposequences, in order to ascertain pedogenetic markers among the attributes studied.

2. Material and methods

2.1. Analytical procedures

Only B horizons were selected for analysis since their characteristics are mainly produced by soil-forming processes. All the analyses were run in triplicate. A variation up to 10% with respect to the average was admitted. The average values of the chemical and electrochemical parameters measured were used to calculate the ratios and statistical analysis.

2.1.1. Particle size distribution

The analysis of particle size distribution was conducted by the pipette method (Soil Survey Staff, 1972).

2.1.2. Bulk density

A cylindrical metal sampler of 55-cm³ volume was pressed horizontally into the soil horizon of each profile and carefully removed to preserve the soil structure. Two 50-cm³ samples of each horizon were dried at 105 °C and weighed. Bulk density was

calculated by dividing the oven-dried mass of the two samples by the 100-cm³ volumes.

2.1.3. Silica sorption and solubility

The index of silica reactivity (ISR) was defined as the percentage of silica lost from a solution brought into contact with the soil (Gallez et al., 1977). The ISR/clay ratio was calculated by correcting the weight of the soil sample by its clay content. The index of silica saturation (ISS) was determined as the ratio of the amount of silica soluble in a 0.05 mol l⁻¹ NaCl extract and the ISR index of a given sample (Herbillon et al., 1977). The equilibrium soil silica activity (pSi(OH)₄) was calculated according to Herbillon et al. (1977).

2.1.4. Specific surface area

The soil surface area was measured by the EGME adsorption procedure (Heilman et al., 1965) according to the modifications proposed by Eltantawy and Arnold (1973), Cihacek and Bremner (1979) and Ratner-Zohar et al. (1983). The procedure is briefly described as follows: samples were slightly ground and passed through a 0.25-mm sieve. EGME was added to about 1 g of oven-dried soil. The slurry was allowed to stand for 1 h. The desiccator (with approximately 30-ml EGME and 200-g CaCl₂ desiccant placed separately) was evacuated for 45 min. The samples were left undisturbed overnight under vacuum (with a maximum of six of samples per desiccator) and then weighed. The desiccator was re-evacuated for 45 min, and samples were allowed to stand under vacuum for 6 h and re-weighed. This procedure was repeated until a constant weigh was achieved, generally after 24 h.

2.1.5. H₂SO₄ dissolution of the clay fraction

The chemical composition of the fine fraction was determined by H₂SO₄ dissolution (Embrapa, 1997), as briefly described: One gram of soil sample was boiled in a H₂SO₄ solution (1:1 by volume) for 30 min. After filtering, the solid portion retained in the filter was used for Si determination, and Al, Fe and Ti analyses of the filtrate were carried out.

Si was extracted by boiling the solid residue in 0.2 mol l⁻¹ NaOH solution for 30 min. Si was determined colorimetrically using ammonium molybdate and ascorbic acid. Fe was determined in the sulfuric

extract by complexometric titration using 0.01 mol l^{-1} EDTA with sulphosalicylic acid as indicator. Al was determined by backtitration. The extract is completed with 0.031 mol l^{-1} EDTA and the excess EDTA titrated with $0.0156 \text{ mol l}^{-1}$ ZnSO_4 . Ti was determined colorimetrically in the extract after the removal of organic matter.

The ratios of Al and Fe obtained by the sulfuric acid dissolution (sa) and the extractants ammonium oxalate (o) or dithionite–citrate–bicarbonate (d) (as Fe_o/Fe_d , $\text{Fe}_o/\text{Fe}_{\text{sa}}$ and $\text{Fe}_d/\text{Fe}_{\text{sa}}$), used as indexes related to the degree of pedogenesis (Blume and Schwertmann, 1969; Anjos et al., 1998), were calculated by simple division.

2.1.6. Electrochemical parameters

ΔpH is expressed by the difference between pH values in 1:1 soil/solution ratios with 1 mol l^{-1} KCl and H_2O .

The point of zero salt effect (PZSE) was determined by the titration method using three different concentrations of KCl (0.1, 0.01, 0.001 mol l^{-1}). The PZSE values were obtained by the pH of the intersection point of the titration curves (Camargo et al., 1986). The following parameters were based on the potentiometric titration curves as well.

- (1) The amount of permanent charge (σ_p) was expressed as the amount of H^+ or OH^- adsorbed at the PZSE (Sakurai et al., 1988);
- (2) The surface net charge (σ) was expressed as the net charge measured at one unit of pH above PZSE in the $10^{-2} \text{ mol l}^{-1}$ KCl titration curve (Pérez et al., 1993).
- (3) The electrical double layer capacity (EDLC) is a thermodynamic concept defined by Bérubé and De Bruyn (1968) and Blok and De Bruyn (1970) for pure crystals. In order to extend this concept to soil, the EDLC was calculated as the ratio of σ and the soil surface area. The factor 163.56 was used to convert $\text{cmol}_c \text{ m}^{-2} \text{ pH}^{-1}$ into coulomb $\text{dm}^{-2} \text{ V}^{-1}$ (Pérez et al., 1993).

2.2. Description of the two study areas

Two toposequences in the state of São Paulo, Brazil, one in Itatiba County and another in Mogi-Guaçu County, were selected for this study. They

were chosen since they have a well developed Oxisol–Ultisol transition along the hillslopes (Moniz and Buol, 1982). Besides, they have been extensively investigated with respect to their morphological characteristics, which are summarized below. A full description can be found elsewhere (Moniz, 1980).

With the introduction of the kandic horizon in Soil Taxonomy (Soil Survey Staff, 1994), some former argillic horizons found in both Itatiba and Mogi-Guaçu sites are now classified as kandic horizons. Kandic horizons can be present in both Ultisols or Oxisols. Clay films may or may not be present in kandic horizons. The argillic and kandic horizons in Ultisols have very similar morphoplogy, their main difference being the apparent cation exchange capacity of the clay. Since this study is focusing on how chemical and electrochemical properties are related to the soil morphological transformation along the two slopes, and considering the morphological similarity between the kandic and argillic horizons, these horizons will be jointly represented as “kandic/argillic” to simplify the discussion.

The main discriminating feature between the Itatiba and the Mogi-Guaçu sites is the greater clay content of the former while the latter consists of medium textured soils. In addition, the Fe_d content averages in the B horizon are higher for profiles 1211, 1212, 1213 and 1214 of the Itatiba toposequence, with 66.2, 77.5, 84.3 and $97.3 \text{ g kg}^{-1} \text{ Fe}_2\text{O}_3$, respectively, than profiles 1215, 1216, 1217 and 1218 of the Mogi-Guaçu toposequence, with 28.4, 39.8, 30.2 and $16.3 \text{ g kg}^{-1} \text{ Fe}_2\text{O}_3$, respectively (Moniz et al., 1982).

In the Itatiba toposequence, the transect begins at a narrow level surface on the crest of the hill and continues down the hillside along a ridge. The mean summer and winter temperatures are 21.8 and 15.9 °C, respectively, the average annual rainfall is 1318 mm and the soil moisture regime is udic. In the Oxisol landscape of Itatiba, a thick granite gneiss saprolite is covered by a incoherent detrial material with oxic properties. Colluvial layers were thicker on the hilltop and at the foot of the slopes but considerably thinner in mid-slope. This is interpreted to be the result of erosion processes. A seepage is found near profile 1214 at the same topographic position as profile 1213, indicating that this profile was formed under a wetter condition than profile 1213.

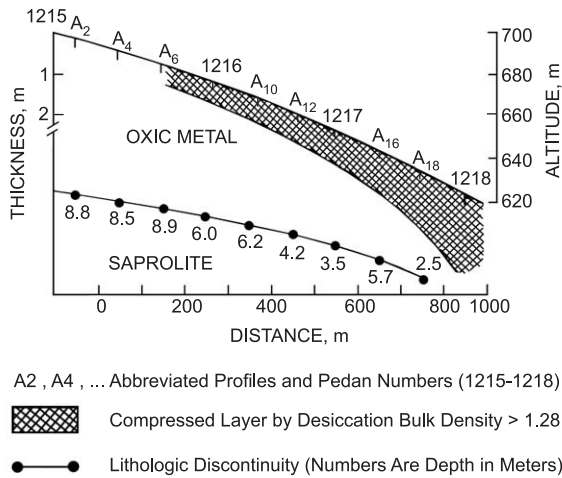


Fig. 1. Cross section in the Mogi-Guaçu toposequence showing the position of the main profiles 1215–1218, indicating the thickness of the compressed layer by desiccation and the lithologic discontinuity. Bulk density in g kg^{-1} (Moniz and Buol, 1982).

The more compressed upper layer of the toposequence in Itatiba presents aggregates with better defined boundaries in a macroscopic visual inspection of the clods. Individual aggregates have numerous flat surfaces which sharply protrude from the clod surface. Argillans are observed in the lower part of the compressed layer of profile 1212 (B1 horizon) and profile 1213 (B1, B21 and IIB22 horizons) (Moniz, 1980). The main feature of the compressed layer is a moderate, fine and medium subangular blocky structure that is also found in the A3 horizon (profiles 1213 and 1214) and even in the surface horizon (profile 1213–A1 horizon).

Aggregates of the compressed layer under wetter conditions have a distinct morphology, mainly in profile 1214. These aggregates are larger and the boundaries are not as well defined as those from the compressed layer of the drier sites along the transect. In profile 1214, argillans are common in field observations throughout the B horizon and smaller amounts of oriented clay are also observed in thin sections of both A subhorizons. Soils in the Itatiba region are mainly low base status Oxisols. Profile 1914 has a high base saturation percentage. The bases were probably supplied by the base-water flow which passed through the interface crystalline rock-saprolite where bases are being released by

primary mineral weathering. The structure of the compressed layer in profiles 1213 and 1214 is water unstable, breaking down completely during the slake test, with vacuum (500 Pa) or without, where the latter reacted faster but with similar final results.

Underlying the compressed layer, oxic material is found with its massive or structureless appearance as usually described in field observations but composed of very fine granules better observed in thin sections under a microscope. Its subrounded peds are not well packed (bulk density about 1 g cm^{-3}), leaving large compound packing voids around the peds.

Soils along the Mogi-Guaçu toposequence are derived from a thick colluvial layer of medium-textured unconsolidated material which gradually becomes thinner down the slope (Fig. 1, Table 1). The colluvial layer is underlined by a Permo–Carbonifero sandstone bedrock easily distinguished in the field by color and consistency. The materials are separated by an almost continuous thin stone line. The sandstone bedrock is altered in situ but retains its particle arrangement.

In the Mogi-Guaçu toposequence, the annual rainfall is 1318 mm and the soil moisture regime is udic. Mean summer and winter temperatures are 22.2 and 16.5 °C, respectively.

Table 1
Soil-landscape characteristics measured in the field of the Itatiba and Mogi-Guaçu toposequences

Profile	Position in the slope	Slope (%)	Shed		Slope length (m)	Thickness of colluvium layer (m)
			Plan	Profile		
<i>Itatiba toposequence</i>						
1211	Crest	3.0	Convex	Convex	0	5.0
1212	Midslope	8.5	Convex	Convex	150	1.5
1213	Footslope	13.0	Slightly convex	Slightly convex	300	3.5
1214 ^a	Footslope	7.0	Concave	Concave	300	4.0
<i>Mogi-Guaçu toposequence</i>						
1215	Crest	1.0	Convex	Convex	0	8.5
1216	Upper Midslope	3.5	Convex	Convex	350	6.0
1217	Lower Midslope	6.0	Convex	Convex	650	3.5
1218	Footslope	7.0	Convex	Convex	900	3.0

^a Placed in a transect parallel to the 1211–1213 transect and 340 m apart.

The subangular blocky structure of aggregates in the compressed layer of the Mogi-Guaçu site is less developed than those of the Itatiba site, although the former is more compacted. The smaller amount of clay (27%) in Mogi-Guaçu soils, less than half of that found in Itatiba soils (64%), is the main determining factor of the structure's grade of development. The lower boundary of the compressed layer in the Mogi-Guaçu toposequence (Fig. 1) cannot be recognized as easily in the field as at the Itatiba site (Moniz, 1980). Few argillans are observed in the lower part of the compressed layer in profiles 1217 and 1218. The aggregates of the compressed layer of the Mogi-Guaçu site are less water stable than those from the Itatiba site. The aggregation in the lower part of the compressed layer in profile 1218 is quickly destroyed when put under vacuum (500 Pa).

All profiles were morphologically described and sampled down to a depth of 200 cm. Based on all available data (Moniz and Buol, 1982), the taxonomic placement (Table 2) was made according to Soil Taxonomy at that time (Soil Survey Staff, 1975). When the kandic horizon was defined in Soil Taxonomy, the argillic horizon of profile 1214 (Soil Survey Staff, 1975) became an Oxisol with becomes a kandic horizon, and the soil is classified as Oxisol (Soil Survey Staff, 1994).

Table 2
Classification of pedons (Moniz and Buol, 1982)

Pedon	Subgroup	Family
<i>Itatiba toposequence</i>		
1211	Haplic Acrorthox	Clayey, kaolinitic, hyperthermic
1212	Typic Acrorthox ^a	Clayey, kaolinitic, hyperthermic
1213	Typic Hapludult ^b	Clayey, kaolinitic, hyperthermic
1214	Typic Paleudalf ^c	Very fine, kaolinitic, hyperthermic
<i>Mogi-Guaçu toposequence</i>		
1215	Haplic Acrorthox	Fine-loamy, siliceous, hyperthermic
1216	Haplic Acrorthox	Fine-loamy, siliceous, hyperthermic
1217	Typic Paleudult	Fine-loamy, siliceous, hyperthermic
1218	Typic Paleudult	Fine-loamy, siliceous, hyperthermic

^a Clay increase enough for argillic but no clay skins.

^b Has clay skins but lacks clay content increase for argillic. Ultisol placement is made on basis of assumed erosion. (Soil Survey Staff, 1975).

^c Reclassified as a kandicidalfic Eutradox by changes in Soil Taxonomy (Soil Survey Staff, 1994).

2.3. Statistics

2.3.1. Principal component analysis

Principal component analysis (PCA) (Ferreira, 2002; Massart et al., 1988; Wold et al., 1987) is one of the most common multivariate methods of data analysis. It can be used for many purposes as, for example, to reveal dominant patterns of the data set. Its aim is to group correlated variables by replacing the original ones by a new set called principal components, PC, onto which the data are projected. These PC are completely uncorrelated and built as a simple linear combination of the original variables. It is important to point out here that the PC contain most of the variability in the data set, albeit in a much lower dimensional space. The first principal component, PC1, is defined in the direction of maximum variance of the whole data set. PC2 is the direction that describes the maximum variance in the subspace orthogonal to PC1. Subsequent components are taken orthogonal to the previously chosen PC and describe the rest of the remaining variance. The data matrix \mathbf{X} ($I \times J$), corresponding to I "samples" or objects and J "variables" (which comprise the measurements made on the objects), is decomposed into two matrices, \mathbf{T} and \mathbf{P} , such that $\mathbf{X} = \mathbf{TP}^T$.

The matrix \mathbf{T} , known as the "scores" matrix, represents the position of the samples in the new coordinate system where the PC are the axes. \mathbf{P} is the "loading" matrix whose columns describe how the new axes, i.e., the PC, are built from the old axes. Scores plots allow insights into sample relationships, displaying their similar, dissimilar, typical or outlier character. The most important variables are identified by the loadings. The higher the individual loading value of a variable in a PC, the more the variable has in common with this component. Small (positive or negative) values indicate a weak relationship between the two.

In this work, the modeling and discriminating power (Wold and Sjostrom, 1977) of the pattern recognition technique soft independent modeling of class analogy (SIMCA), whose principle is based on PCA, was also used for variable selection. The SIMCA method builds principal component models for each class (each profile). The number of optimal PC is determined for each class and the model is completed by defining boundary regions for each

Table 3

Chemical and electrochemical attributes of B horizons from the Itatiba toposequence used for PCA and HCA analysis

Soil		Variables ^a									
Profile	Horizon	ΔpH	Clay (g kg^{-1})	Bulk density (g cm^{-3})	SSA ($\text{m}^2 \text{g}^{-1}$)	ISS	ISR (%)	ISR/Clay	PZSE	σ ($\text{cmol}_c \text{kg}^{-1}$)	σ_p
1211d	B1	-0.6	690	1.06	80	16	73	106	4.00	0.85	0.70
1211e	B21	-0.6	650	0.93	90	20	70	108	4.00	0.85	0.60
1211f	B22	-0.1	740	0.99	87	22	75	101	4.04	0.85	0.60
1211g	B23	0.1	690	1.10	75	18	77	112	5.75	0.50	-0.50
1211h	B24	0.5	740	1.10	72	14	74	100	6.24	0.65	-0.70
1212c	B1	0.6	640	1.23	66	12	70	109	4.32	0.85	0.60
1212d	B21	0.7	620	1.04	64	16	65	105	4.43	0.80	0.65
1212e	IIB31	0.3	560	1.14	57	19	64	114	6.85	0.65	-1.10
1212f	IIB32	0.0	550	1.16	51	26	62	113	5.20	0.80	-0.30
1213c	B1	-0.2	640	1.22	81	52	68	106	4.25	0.70	0.20
1213d	B21	-0.4	650	1.26	97	50	71	109	4.28	0.80	0.20
1213e	IIB22	0.0	660	1.25	108	39	77	117	4.52	0.60	0.10
1213f	IIB23	0.3	610	0.93	73	41	69	113	5.40	0.60	-0.30
1213g	IIIB24	0.9	670	1.09	101	22	71	106	6.30	0.50	-0.60
1213h	IIIB25	0.6	740	1.10	98	15	75	101	6.65	0.80	-0.80
1213i	IIIB26	0.5	720	1.20	73	17	73	101	7.00	1.20	-0.90
1214c	B21	-0.6	690	1.37	91	61	58	84	3.75	1.80	2.30
1214d	B22	-0.3	700	1.24	98	58	63	90	3.80	1.40	2.00
1214e	B23	-0.2	650	1.27	93	57	61	94	3.90	1.50	2.00
1214f	B3	-0.7	670	1.19	74	54	63	94	3.80	1.40	2.00

Soil		Variables ^b							
Profile	Horizon	EDLC ^c	$\text{Fe}_d/\text{Fe}_{\text{sa}}$	$\text{Fe}_o/\text{Fe}_{\text{sa}}$	Fe_o/Fe_d	$\text{pSi}/\text{Si}_{\text{sa}}$	$\text{Al}_d/\text{Al}_{\text{sa}}$	$\text{Al}_o/\text{Al}_{\text{sa}}$	Al_o/Al_d
1211d	B1	1.74	0.715	0.019	0.027	4.16	0.102	0.404	0.395
1211e	B21	1.55	0.684	0.021	0.031	4.11	0.099	0.392	0.395
1211f	B22	1.60	0.718	0.016	0.022	4.06	0.108	0.280	0.259
1211g	B23	1.08	0.670	0.014	0.020	4.09	0.096	0.271	0.282
1211h	B24	1.48	0.694	0.014	0.020	4.22	0.094	0.220	0.235
1212c	B1	2.12	0.619	0.010	0.016	4.42	0.060	0.193	0.321
1212d	B21	2.05	0.691	0.009	0.014	4.35	0.070	0.213	0.306
1212e	IIB31	1.86	0.691	0.009	0.014	4.30	0.063	0.230	0.363
1212f	IIB32	2.59	0.671	0.008	0.011	4.19	0.040	0.143	0.360
1213c	B1	1.41	0.672	0.021	0.031	3.76	0.11	0.23	0.22
1213d	B21	1.35	0.675	0.018	0.027	3.76	0.10	0.24	0.23
1213e	IIB22	0.91	0.694	0.017	0.024	3.80	0.11	0.28	0.25
1213f	IIB23	1.35	0.671	0.018	0.027	3.90	0.11	0.24	0.23
1213g	IIIB24	0.81	0.672	0.017	0.025	4.10	0.10	0.19	0.20
1213h	IIIB25	1.33	0.732	0.021	0.028	4.28	0.09	0.16	0.17
1213i	IIIB26	2.68	0.710	0.021	0.030	4.28	0.09	0.16	0.18
1214c	B21	3.24	0.701	0.019	0.026	3.73	0.100	0.174	0.173
1214d	B22	2.35	0.713	0.018	0.025	3.79	0.112	0.178	0.158
1214e	B23	2.65	0.688	0.019	0.028	3.74	0.102	0.179	0.175
1214f	B3	3.11	0.717	0.021	0.029	3.77	0.109	0.210	0.193

^a $\Delta\text{pH}=\text{pH KCl}-\text{pH H}_2\text{O}$, SSA: specific surface area, ISS: index of silica saturation, ISR: index of silica reactivity, PZSE: point of zero salt effect, σ : surface net charge, σ_p : amount of permanent charge.

^b EDLC: electrical double layer capacity, d: dithionite–citrate–bicarbonate extraction, o: ammonium oxalate extraction, sa: sulphuric acid extraction.

^c Coulomb $\text{dm}^{-2} \text{V}^{-1}$.

PCA model. In other words, a hyperbox is constructed for each class. The modeling power of a variable is defined as $MP=1-s_j^2/s_{0j}^2$, where s_j^2 is the variable residual variance and s_{0j}^2 the total variance of that variable. A value of MP close to one indicates a high modeling power. The discriminating power (DP) of a variable between two classes was calculated consid-

ering the residual standard deviation of the samples of a given class when fitted to other classes. A DP close to zero indicates that a variable has not enough discrimination power to distinguish between classes.

Another crucial point to be considered in data analysis is preprocessing. The original data matrix usually does not present an optimal value distribution

Table 4

Chemical and electrochemical attributes of B horizons from Mogi-Guaçu toposequence used for PCA and HCA analysis

Soil			Variables ^a								
Profile	Horizon	ΔpH	Clay (g kg ⁻¹)	Bulk density (g cm ⁻³)	SSA (m ² g ⁻¹)	ISS	ISR (%)	ISR/Clay	PZSE	σ (cmol _c kg ⁻¹)	σ_p
1215c	B1	-0.2	300	1.06	31	58	83	277	3.85	0.55	0.30
1215d	B21	-0.2	310	0.98	28	66	84	271	4.04	0.60	0.30
1215e	B22	0.0	320	1.01	34	75	89	278	3.20	0.70	0.65
1215f	B23	0.1	340	1.05	47	72	93	274	3.76	0.60	0.50
1216c	B1	-0.5	300	1.25	45	40	94	313	3.60	0.95	1.05
1216d	B21	-0.7	300	1.22	37	59	83	277	3.81	0.70	0.50
1216e	B22	-0.7	340	1.19	34	86	83	244	3.85	0.70	0.50
1216f	B23	-0.4	350	1.21	39	76	85	243	3.90	0.55	0.40
1217c	B1	-0.9	300	1.29	35	34	86	287	3.65	0.95	0.80
1217d	B21	-0.8	310	1.21	31	40	80	258	3.50	0.90	0.80
1217e	B22	-0.7	320	1.25	32	57	81	253	3.90	0.75	0.55
1217f	B3	-0.5	310	1.27	33	69	76	245	3.92	0.85	0.75
1218c	B1	-0.6	200	1.39	29	33	72	360	3.40	1.05	1.00
1218d	B21	-0.9	220	1.51	34	35	70	318	3.25	1.10	1.00
1218e	B22	-0.7	250	1.50	35	38	71	284	3.30	1.10	1.00
1218f	B3	-0.8	220	1.70	33	52	61	277	3.45	1.00	0.70

Soil		Variables ^b								
Profile	Horizon	EDLC ^c	Fe _d /Fe _{sa}	Fe _o /Fe _{sa}	Fe _o /Fe _d	pSi/Si _{sa}	Al _d /Al _{sa}	Al _o /Al _{sa}	Al _o /Al _d	
1215c	B1	2.87	0.768	0.030	0.039	3.24	0.105	0.343	0.327	
1215d	B21	3.56	0.759	0.024	0.032	3.19	0.099	0.309	0.312	
1215e	B22	3.36	0.684	0.023	0.034	3.16	0.121	0.299	0.246	
1215f	B23	2.09	0.491	0.017	0.035	3.19	0.114	0.263	0.232	
1216c	B1	3.45	0.730	0.030	0.040	3.38	0.093	0.314	0.336	
1216d	B21	3.12	0.786	0.026	0.033	3.23	0.112	0.289	0.258	
1216e	B22	3.38	0.791	0.023	0.029	3.13	0.109	0.256	0.235	
1216f	B23	2.33	0.548	0.021	0.039	3.18	0.133	0.228	0.172	
1217c	B1	4.44	0.797	0.029	0.036	3.44	0.135	0.231	0.171	
1217d	B21	4.69	0.785	0.021	0.026	3.38	0.143	0.206	0.144	
1217e	B22	3.82	0.769	0.023	0.030	3.27	0.089	0.223	0.250	
1217f	B3	4.20	0.750	0.018	0.023	3.24	0.098	0.191	0.194	
1218c	B1	5.83	0.738	0.057	0.077	3.41	0.119	0.319	0.267	
1218d	B21	5.23	0.642	0.042	0.065	3.36	0.124	0.268	0.216	
1218e	B22	5.10	0.680	0.036	0.053	3.46	0.090	0.267	0.296	
1218f	B3	4.99	0.752	0.030	0.040	3.35	0.099	0.262	0.265	

^a $\Delta pH=pH\ KCl-pH\ H_2O$, SE: specific surface area, ISS: index of silica saturation, ISR: index of silica reactivity, PZSE: point of zero salt effect, σ : surface not charge, σ_p : amount of permanent charge.

^b EDLC: electrical double layer capacity, d: dithionite–citrate–bicarbonate extraction, o: ammonium oxalate extraction, sa: sulphuric acid extraction.

^c Coulomb dm⁻² V⁻¹.

for the analysis (for example, has different units and variances in variables), which requires some pretreatment prior to data analysis. In this work, autoscale preprocessing is used, which results in scaled variables with zero mean and unit variance.

2.3.2. Cluster analysis

Hierarchical cluster analysis (HCA) is another important multivariate method of data analysis. Its primary purpose is to display the data so they emphasize its natural clusters and patterns. The results of qualitative nature are presented in the form of a dendrogram allowing the visualization of samples or variables in 2D space. In this method, the distances between samples or variables are calculated and transformed into a similarity matrix **S** whose elements are the similarity indexes. For any two samples k and l , the similarity index is defined as $S_{kl}=1.0-((d_{kl})/(d_{\max}))$, where S_{kl} is an element of **S**, d_{\max} is the largest distance for any pair of samples in the data set. d_{kl} is the Euclidean distance between samples k and l . The similarity scale ranges from zero to one. It is clear that the larger the S_{kl} index, the smaller the distance between k and l . Therefore, S_{kl} reflects their similarity directly. The incremental clustering technique, which employs a sum of squares approach to calculate the nearest cluster, weighted by the cluster population, was used in this work (Massart et al., 1988).

The raw data consisted of 16 variables measured in 36 samples and were autoscaled prior to analysis. The data analysis was carried out on Pirouette statistical software by Infometrix (Seattle, WA, USA).

3. Results

3.1. Distribution pattern of the data

The results of the 16 chemical and electrochemical parameters (referred to as attributes or variables in this work) measured in the 2 toposesquences of Itatiba and Mogi-Guaçu are listed in Tables 3 and 4, respectively.

Before applying the PCA to the soil data, a screening analysis was carried out to visualize the distribution pattern of the studied soil parameters from the top of the hill down to the bottom.

A few variables such as σ , σ_p , EDLC, in the Mogi-Guaçu site as well as ISS in the Itatiba site increased down the slope, while the values of ISS and ISR at the Mogi-Guaçu site decreased down the slope. Many of the variables do not present a regular pattern in the dataset. In some cases, a pattern seems to occur but it is broken by some profiles, which represent a displacement that would not fit the set. These observations made the need for more elaborate techniques such as applied multivariate methods to describe clearly the soil transformation process in focus.

4. Discussion

4.1. Removal of six highly correlated variables from the PCA model

The evaluation of the transformation process was performed by the analysis of statistical information obtained from PCA through the scores and loading plots. As mentioned in the experimental section, the points in the scores plots represent the soils analyzed in the soil profiles of the two toposesquences, and the loadings, the analyzed variables (attributes). A clear discrimination between the Itatiba and Mogi-Guaçu toposesquences was obtained by the application of PCA to the autoscaled data of Tables 3 and 4. Since the objective of this paper was to study the transformation of an oxic into a kandic/argillic transition in the two toposesquences in São Paulo, Brazil, the identification of attributes related to this soil development process among the measured chemical and electrochemical properties was necessary.

In a first step, variables of the dataset were selected for exclusion by determining which pair of chemical and electrochemical variables clearly presented a linear tendency and high correlation coefficients ($r>0.75$). Considering that the chemical information described by highly correlated attributes is approximately the same, one from each set of the correlated variables shown in Table 5 was selected for further analysis, and six involved attributes were excluded. The selected variables were: $\text{Fe}_o/\text{Fe}_{\text{sa}}$, ISS, PZSE and SSA, which joined the variables ISR, σ , $\text{Fe}_d/\text{Fe}_{\text{sa}}$, $\text{Al}_d/\text{Al}_{\text{as}}$, $\text{Al}_o/\text{I}_{\text{sa}}$ and Al_o/Al_d . Thus, the initial 16 attributes were reduced to 10.

Table 5
Sets of variables highly correlated

Set	Variables ^a	Correlation coefficient
1	Fe_o/Fe_{sa} , Fe _o /Fe _d	0.9714
2	ISS , pSi/Si _{sa}	−0.8385
3	ΔpH, PZSE	0.7615
	σ _p , PZSE	−0.7982
4	EDLC, SSA	−0.7677
	ISR/clay, SSA	−0.8746
	EDLC, ISR/clay	0.7848
	ISR _{arg} , pSi/Si _{sa}	−0.8393

^a Selected variables are in bold.

4.2. SIMCA analysis and PCA model for seven variables

Further variable selection was performed using the modeling and discriminating power of each variable, calculated by the SIMCA method (Wold and Sjöström, 1977).

Each soil profile was therefore considered a class that could be described by a two PC model and the residual standard deviation for each class was calculated. Modeling and the discriminating power of the 10 variables are listed in Table 6. Three of these were excluded due to their low modeling and discriminating power. The remaining (ISR, ISS, SSA, Fe_o/Fe_{sa}, Al_o/Al_{sa}, σ and PZSE) are those variables which simultaneously present good modeling and discriminating power. This suggests that chemical and electrochemical attributes were essential to explain the transformation of an oxic into an argillic horizon, since both attributes were selected based on SIMCA analysis.

A PCA was carried out in this set of seven variables, after autoscaling the data and, as a result, 40% of data variance was explained by the first principal component (PC1) and 24% by the second (PC2). The loading plot for PC1xPC2 is shown in Fig. 2. Except for σ, all the variables are heavily loaded in PC1. On the other hand, compared to the other variables, σ is the only variable with a high positive loading in PC2, while ISR and PZSE have moderate negative loadings.

The most appealing characteristic of the scores map shown in Fig. 3 is the clear separation of the two toposequences, which can be attributed to PC1, where the soil profiles of the Mogi-Guaçu site appear on the right and of the Itatiba site on the left side. This means

that the linear combination of the variables of greater weight, described above, allowed PC1 to clearly discriminate these two toposequences. The main difference in both sites stems from higher values for SSA and PZSE and lower values of ISS, ISR, Fe_o/Fe_{sa} and Al_o/Al_{sa} at the Itatiba site in comparison to the Mogi-Guaçu site (Fig. 2).

In addition to this, for Mogi-Guaçu soil profiles, going from soil horizon c to f, more specifically c, d and f, the scores become smaller in PC1 (see Fig. 3). This distribution observed in the scores map can be explained by changes in the loadings from Fig. 2, with a decrease of Fe_o/Fe_{sa} and Al_o/Al_{sa} values, while SSA or PZSE increased, which seems to be occurring with an increase in the depth of the horizons c to f. Also in Fig. 3, it can be seen that PC2 allowed the detachment of the profile 1214 from the others in the upper part of the map. From Fig. 2, it can be noted that the variable σ has an important role in this profile.

The scores map of Fig. 3 shows that the seven selected soil attributes allowed the separation of most soil horizons from the others except for profile 1213. According to Fig. 2, after autoscaling the attribute values and taking the relative weight of such attributes on the discrimination of the profiles into account, the conclusion can be drawn that the separation of profiles 1215 to 1218 in the Mogi-Guaçu toposequence is due to the increase in σ and Fe_o/Fe_{sa} (high positive loadings in PC2) measurements and the simultaneous decrease in ISR, ISS and Al_o/Al_{sa} values (high negative loadings in PC2). Lateral and basal water

Table 6
Discriminating power and modeling power for a 2PC model for soil profiles using SIMCA^a

Variables ^b	Discriminating power	Total modeling power
SSA	906.78	0.76
ISS	274.90	0.79
ISR	139.180	0.80
PZSE	645.76	0.72
σ	95.72	0.78
Fe _d /Fe _{sa}	61.58	0.71
Fe_o/Fe_{sa}	422.93	0.85
Al _o /Al _{sa}	59.20	0.76
Al_o/Al_{sa}	108.28	0.86
Al _o /Al _d	45.47	0.73

^a Data was locally autoscaled.

^b Selected variables are in bold.

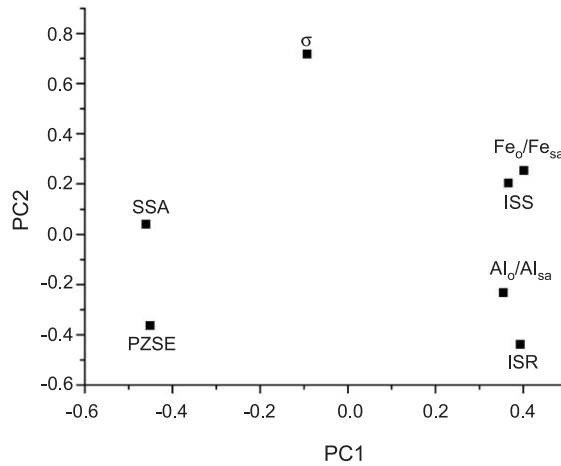


Fig. 2. Loadings map (PC1×PC2) for the PCA with the seven selected variables, after elimination of highly correlated variables.

flow increases down the slope, therefore the transformation in this direction is more expressive, as shown in Fig. 1. Furthermore, Fig. 3 demonstrates that, from the bottom to the top of the scores map, profile separation followed the increase of the kandic/argillic horizon development, similar to the soil distribution along the slope, with a larger separation of profiles 1218 and 1214, both with highest soil development.

Although profile 1213 of the Itatiba site in the scores map of Fig. 3 has a kandic/argillic horizon, it

was not located close to profile 1214, but overlapped with the profiles 1211 and 1212. The kandic/argillic horizon of profile 1213 was developed on a slight convex slope in both plain and profile which did not favor its development, in contrast to profile 1214, which presented a concave slope both in plain and in profile. The latter presented more ideal moisture conditions for soil development than the former. In profile 1213, horizons c, d, e and f are grouped together with profile 1211, but horizons g, h and i are well separated from the previous ones, although

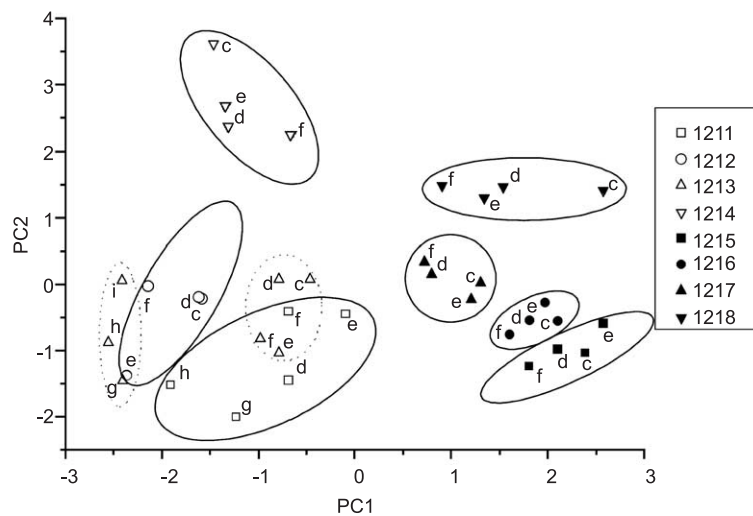


Fig. 3. Scores map (PC1×PC2) for the PCA with the seven selected variables, after elimination of highly correlated variables.

they present some similarity with soils in profile 1212. Based on the loading map (Fig. 2), this seems to be due to the PZSE values (Table 3) increasing with depth (profile 1213).

In the clayey soils of the Itatiba toposequence, the highest ISS value is observed in the most juvenile soil (profile 1214) with lower ISS in the older ones (profiles 1211 and 1212), as expected according to Herbillon et al. (1977). The slight separation of profiles 1211/1212 and 1215/1216 (oxic horizons) at each toposequence was very meaningful, since it indicates an incipient alteration in those soils due to the action of the lateral water flow even in the upper part of the slope. In profile 1213, the ISS values of soil horizons from both parent materials I and II are closer to profile 1214, while in the horizons of profile 1213 derived from the deepest parent material III, the ISS values are similar to profiles 1211 and 1212. This could be an indication, according to the slope characteristics, that the amount of moisture was not sufficient to promote a deeper alteration in those deepest soil horizons, which could explain the horizon distribution of profile 1213 in Fig. 3.

4.3. PCA model and HCA without profile 1213

Profile 1213 was removed from the analysis for a better visualization in the scores plot due to its development from three soil materials, each at a

different stage of development, as indicated by the chemical and electrochemical properties.

The scores plot of PCA and the dendrogram of HCA excluding profile 1213 are shown in Figs. 4 and 5. As expected, the removal of profile 1213 also gave rise to more consistent results, producing tighter horizon groups for each soil profile in both PCA and HCA. Profile 1214, in the same topographic position as profile 1213 and on the same slope in a transect parallel to transect 1211–1213, 340 m apart, with a more developed argillic horizon, replaced profile 1213 satisfactorily and maintained the three positions in the slope, without affecting the results.

The PCA scores for the first two PC, which explains 65.6% of the total variance, are shown in Fig. 4. The first PC, accounting for 39.2% of the total data variance, clearly describes the different toposequences and the profiles along the foot of the slopes by the relative weight in the loadings described in Fig. 2. The second PC, which accounts for 26.4% of the variance, describes the higher degree of the kandic/argillic horizon development through the variables σ and ISR (profiles 1214 and 1218), located apart from the other profiles (Figs. 4 and 5).

It should be noted that the seven attributes used in the PCA were found to be essential to obtain the best discrimination among soil profiles in the toposequences. The exclusion of any of the attributes, even attributes such as Fe_o/Fe_{sa} and Al_o/Al_{sa} that do not

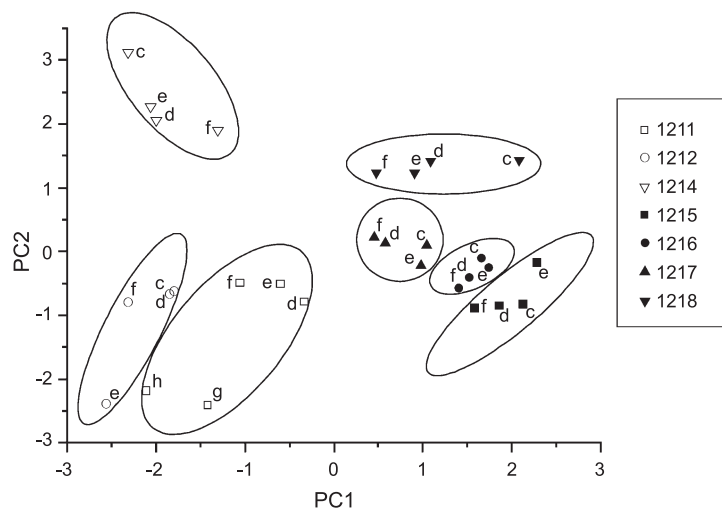


Fig. 4. Scores map (PC1×PC2) for the PCA with the variables σ , ISR, ISS, PZSE, SSA, Fe_o/Fe_{sa} , Al_o/Al_{sa} .

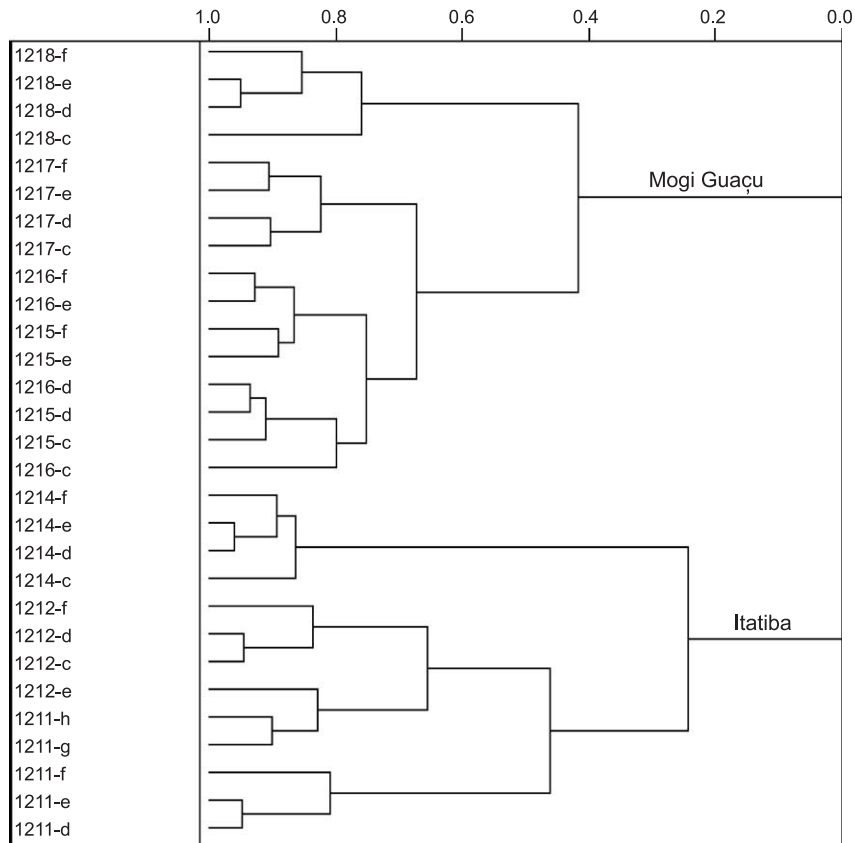


Fig. 5. HCA for soil horizon data using the variables σ , ISR, ISS, PZSE, SSA, Fe_o/Fe_{sa} , Al_o/Al_{sa} .

present a clear regular pattern in the original data (Tables 3 and 4), were found to be important for the discrimination of profile 1215 from 1216 or of 1217 from 1218 by the statistical methods employed. In addition to this, one should emphasize that chemical and electrochemical attributes measured for this pedological transformation system were obtained from almost ideal conditions due to the similarities among the four soil forming factors of each toposequence (parent material, relief, climate, organisms), though kandic/argillic horizons are considered by some pedologists younger than oxic horizons. The similarity in parent material was highly relevant due to the occurrence of a gradual transition of an oxic to a kandic/argillic horizon. The oxic horizon, starting point of the entire transformation, was well characterized.

As already observed in the PCA analysis, the HCA was able to distinguish two main clusters, related to

both sites (Fig. 5). The cluster analyses of profiles 1214, 1218 and 1217 were well defined within each block, presenting the best differentiation for each toposequence. Based on the selected variables, these profiles are the most characteristic of each toposequence, while the others are more similar with each other. The separation of profiles 1211 and 1212 is clearer than of 1215 and 1216. In the dendrogram shown in Fig. 5, the sets of soil horizons of profiles 1215 and 1216 are linked together at a level of 0.75, which means that these soil profiles presented a similarity of 75% when seven variables were used in the analysis, while of the soils in profiles 1211 and 1212 only sample 1212e was allocated in another cluster. All these profiles presented oxic horizons. The relief of profile 1212 had a slope of 8.5%, located at a distance of 150 m from the crest (P-1211) (Table 1). The relief of profile 1216 had a slope of 3.5% and was located 350 m from

the crest (P-1215). The clay ratios B21/A1 for profiles 1212 and 1216 were 1.15 and 1.45, respectively.

The magnitude and direction of the downhill water infiltration flow depends on the degree of anisotropy as well as on the land slope and its changes (Zaslavsky and Rogowski, 1969). The slightly more distinct separation between profiles 1211/1212 in relation to profiles 1215/1216 was probably due to two features: greater slope and higher clay content of the former. The vertical anisotropy estimated by the clay ratio probably had a minor effect.

5. Conclusion

Moniz and Buol (1982) studied soil morphology behavior based on principles of soil mechanics to explain Oxisol–Ultisol relationships in two very common toposequences of the Brazilian landscape. The present data suggested, by the use of multivariate statistical methodology (PCA and HCA), that seven chemical/electrochemical soil properties were essential to explain the transformation of an oxic into an argillic/kandic horizon downslope. This allowed a comprehensive description of the physico-chemical processes that occur simultaneously with the morphological transformation along the toposequences.

Acknowledgements

The authors acknowledge Dr. M. de M. Valeriano and Dr. R.M. Coelho for their valuable suggestions. The authors are also grateful to Prof. C.H. Collins for reading the manuscript.

References

- Anjos, L.H., Fernandes, M.R., Pereira, M.G., Franzmeier, D.P., 1998. Landscape and pedogenesis of an Oxisol–Inceptisol–Ultisol sequence in southeastern Brazil. *Soil Sci. Soc. Am. J.* 62, 1651–1658.
- Bérubé, Y.G., De Bruyn, P.L., 1968. Adsorption at the rutile–solution interface: I. Thermodynamic and experimental study. *J. Colloid Interface Sci.* 27, 305–318.
- Blok, L., De Bruyn, P.L., 1970. The ionic double layer at the ZnO/solution interface: III. Comparison of calculated and experimental differential capacities. *J. Colloid Interface Sci.* 32, 533–538.
- Blume, H.P., Schwertmann, U., 1969. Genetic evaluation of the profile distribution of aluminum, iron and manganese oxides. *Soil Sci. Soc. Am. Proc.* 33, 438–444.
- Camargo, O.A., Moniz, A.C., Jorge, J.A., Valadares, J.M.A.S., 1986. Métodos de análise química, mineralógica e física dos solos usados no Instituto Agronômico. *Boletim Técnico* vol. 106. Instituto Agronômico de Campinas, Campinas, Brazil.
- Cihacek, L.J., Bremner, J.M., 1979. A simplified ethylene glycol monoethyl ether procedure for assessment of soil surface area. *Soil Sci. Soc. Am. J.* 43, 821–822.
- Curi, N., Franzmeier, D.P., 1984. Toposequence of Oxisols from the Central Plateau of Brazil. *Soil Sci. Soc. Am. J.* 48 (2), 341–346.
- Eltantawy, I.M., Arnold, P.W., 1973. Reappraisal of ethylene glycol mono-ethyl ether (EGME) method for surface area estimations of clays. *J. Soil Sci* 24, 232–238.
- Embrapa, 1997. Manual de Métodos de Análise de Solo. EMBRAPA-CNPq, Rio de Janeiro, Brazil.
- Ferreira, M.M.C., 2002. Multivariate QSAR. *J. Braz. Chem. Soc.* 13, 742–753.
- Gallez, A., Herbillon, A.J., Juo, A.S.R., 1977. Characteristics of silica sorption and solubility as parameters to evaluate the surface properties of tropical soils: I. The index of silica reactivity. *Soil Sci. Soc. Am. J.* 41, 1146–1150.
- Heilman, M.D., Carter, D.I., Gonzalez, C.L., 1965. The ethylene glycol monoethyl ether (EGME) technique for determining soil-surface area. *Soil Sci.* 100, 409–413.
- Hendershot, W.H., Lavkulich, L.M., 1978. The use of zero point of charge (ZPC) to access pedogenic development. *Soil Sci. Soc. Am. J.* 42, 468–472.
- Herbillon, A.J., Gallez, A., Juo, A.S.R., 1977. Characteristics of silica sorption and solubility as parameters to evaluate the surface properties of tropical soils: II. The index of silica saturation. *Soil Sci. Soc. Am. J.* 41, 1151–1154.
- Massart, D.L., Vandeginste, B.G.M., Deming, S.N., Michotte, Y., Kaufman, L., 1988. *Chemometrics: A Textbook*. Elsevier, Amsterdam.
- Moniz, A.C., 1980. Formation of an Oxisol–Ultisol transition in São Paulo, Brazil. Ph.D thesis. Department of Soil Science, North Carolina State University at Raleigh.
- Moniz, A.C., Buol, S.W., 1982. Formation of an Oxisol–Ultisol transition in São Paulo, Brazil: I. Double-water flow model of soil development. *Soil Sci. Soc. Am. J.* 46, 1228–1233.
- Moniz, A.C., Buol, S.W., Weed, S.B., 1982. Formation of Oxisol–Ultisol transition in São Paulo, Brazil: II. Lateral dynamics of chemical weathering. *Soil Sci. Soc. Am. J.* 46, 1234–1239.
- Pérez, D.V., Ramos, D.P., Nascimento, R.A.M., Barreto, W.O., 1993. Propriedades eletroquímicas de horizontes B texturais. *Rev. Bras. Cienc. Solo* 17, 157–164.
- Ratner-Zohar, Y., Banin, A., Chen, Y., 1983. Oven drying as a pretreatment for surface-area determinations of soils and clays. *Soil Sci. Soc. Am. J.* 47, 1056–1058.
- Sakurai, K., Ohdate, Y., Kyuma, K., 1988. Comparison of salt titration and potentiometric titration methods for the determination of zero point of charge (ZPC). *Soil Sci. Plant Nutr.* 34, 171–182.

- Schaefer, C.E.R., Ker, C., Gilkes, R.J., Campos, J.C., da Costa, L.L., Saadi, A., 2002. Pedogenesis on the uplands of the Diamantina Plateau, Minas Gerais, Brazil: a chemical and micropedological study. *Geoderma* 107 (3–4), 243–269.
- Soil Survey Staff, 1972. Soil Survey Laboratory Methods and Procedures for Collecting Soil Samples. Report No. 1. U.S. Department of Agriculture United States Government Printing Office, Washington, DC. 63 pp.
- Soil Survey Staff, 1975. Soil taxonomy. A Basic System of Soil Classification for Making and Interpreting Soil Surveys, Agriculture Handbook vol. 436. U.S. Department of Agriculture, U.S. Government Printing Office, Washington, DC.
- Soil Survey Staff, 1994. Keys to Soil Taxonomy. Sixth Edition. Natural Resources Conservation Service. U.S. Department of Agriculture, Government Printing Office, Washington, DC.
- Wold, S., Sjostrom, M., 1977. IN: Chemometrics: Theory and Application. In: Kowalski, B.R. (Ed.), ACS Symposium Series, 52 ed. American Chemistry Society, Washington, DC, pp. 243–282.
- Wold, S., Esbensen, K., Geladi, P., 1987. Principal component analysis. *Chemom. Intell. Lab. Syst.* 2, 37–52.
- Zaslavsky, D., Rogowski, A.S., 1969. Hydraulic and morphologic implications of anisotropy and infiltration in soil profile development. *Soil Sci. Soc. Am. Proc.* 33, 594–599.